New Fault-Location Algorithm for Transmission Lines Including Unified Power-Flow Controller

Mahdi Ghazizadeh Ahsaee and Javad Sadeh, *Member, IEEE*

***Abstract*—In this research, a novel fault-location algorithm for transmission lines including the unified power-flow controller (UPFC) is proposed. Since this method does not utilize model of the UPFC, the errors resulting from the fault interval model of the UPFC are avoided. In addition, the new technique does not require proposing a selector to select fault section with respect to the UPFC location. This method uses synchronous data gathered from both ends of the transmission line and takes advantage of the distributed parameter line model in time domain. One quadratic equation is obtained, assuming that the fault is located on the left-hand side of the UPFC. The same procedure is applied for the assumed fault on the right-hand side of the UPFC and another quadratic equation is achieved. These two equations are used to derive an optimization problem that the location of fault is calculated by solving this problem. A 300-km/500-kV transmission line, including a UPFC simulated in MATLAB/Simulink, has been used to evaluate the performance of the new method. The obtained results show the accuracy of the proposed algorithm.**

***Index Terms*—Distributed parameter line model, fault location, synchronous sampling, time domain, unified power-flow controller (UPFC).**

I. Introduction

PROPOSING fault-location algorithms for transmission lines is still a subject of great interest to researchers and utilities. Fault location is required to make necessary repairs and to expedite service restoration.

The unified power-flow controller (UPFC) is the most influential of the flexible ac transmission systems (FACTS) and by means of an angularly unconstrained series injected voltage, is able to control, concurrently or selectively, the transmission-line impedance, the terminal voltage magnitude, and the active and reactive power flow through it [1], [2]. These basic capabilities make it the most powerful device for transmission-lines control and to enhance transient stability, voltage stability, and dynamic stability of the system.

When a fault occurs, the presence of the FACTS devices in the line creates new problems for fault-location algorithms and since the control system of these devices reacts to the fault, the voltages and currents used by the fault locator will be affected in the transient state. Several fault-location methods are proposed for transmission lines in the presence of compensators and FACTS devices [3]–[9], which can be categorized into two groups. The first group [3]–[6] uses the compensator model to find the location of fault, and the second group [7]–[9] does not utilize the compensator model. Fault-location algorithms for transmission lines in the presence of UPFC are presented in few articles, such as [6], where the UPFC model is used and this method includes inherent errors depending on its model. One difficulty with such algorithms is choosing the fault interval model of the UPFC and determining its parameters on which the accuracy of these methods depends. Obviously, choosing an unsuitable fault interval model and parameters for the UPFC may cause large errors in results. On the other hand, in [6], the lumped model of the line is taken into account. However, the distributed parameter line model in the time domain models the line more accurately and is more suitable for the fault-location studies. Also, the method presented in [6] uses a wavelet-fuzzy discriminator to select the correct section of the fault with respect to the UPFC location before fault-location estimation.

The objective of the work presented in this paper is to propose a new fault-location method for transmission lines in the presence of the UPFC. In order to overcome the difficulties of the UPFC modeling during faults, the UPFC model is not used in the algorithm. Consequently, the errors resulting from the modeling of the UPFC are removed. In addition, this algorithm unlike [6] does not require proposing a selector to determine the faulty section with respect to the UPFC location. In this algorithm, distributed parameter line model in time domain is employed and synchronous voltage and current data from both ends of transmission line are utilized. Two quadratic equations assuming that the fault is once located on the left and once on the right-hand side of the UPFC are obtained which are used to derive an optimization problem. The location and resistance of the fault are determined by solving this optimization problem. A typical transmission line compensated by a UPFC at the middle has been used to evaluate the performance of the proposed algorithm.

The rest of this paper is organized as follows. The next part of this paper (Section II) explains the proposed fault-location method for transmission lines including UPFC. Then, in Section III, the results of MATLAB/Simulink simulation-based evaluation of the developed fault-location algorithm are presented and discussed. Conclusions are finally made in Section IV.

II. Proposed Fault-Location Method

Fig. 1 depicts a transmission line including a UPFC in which a three-phase fault occurs on the left-hand side of the UPFC at point F, at a distance x from the sending end. Systems A and B represent Thevenin's equivalent of the external networks. S

Manuscript received January 26, 2011; revised July 02, 2011; accepted May 19, 2012. Date of publication July 12, 2012; date of current version September 19, 2012. Paper no. TPWRD-00074-2011.

The authors are with the Electrical Engineering Department, Faculty of Engineering, Ferdowsi University of Mashhad, Mashhad 9177948944, Iran (e-mail: mahdi_ghazy@yahoo.com; sadeh@ieee.org).

Digital Object Identifier 10.1109/TPWRD.2012.2202404

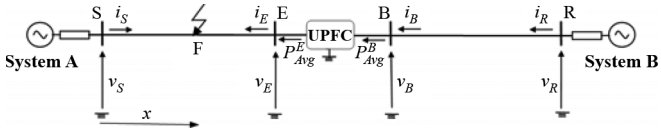

Fig. 1. Single-line diagram of transmission line including UPFC. The fault occurs on the left-hand side of the UPFC.

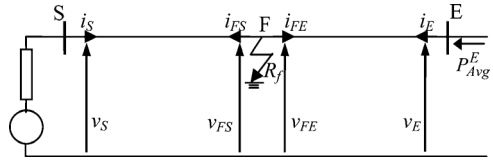

Fig. 2. Single-line diagram of the SE section of the transmission line with distributed parameters.

and R represent sending and receiving end buses, respectively. Since the BR section of the line is sound, the voltage and current vectors at the right-hand side of the UPFC $(\mathbf{v_B}, \mathbf{i_B})$ can be calculated using the receiving end voltage and current vectors $(\mathbf{v_R}, \mathbf{i_R})$. For the faulty section of the line (SE section), the voltage and current vectors of bus $\mathbf{S}(\mathbf{v_S}, \mathbf{i_S})$ are known and the voltage and current of bus $\mathbf{E}(\mathbf{v_E}, \mathbf{i_E})$ are unknown. Therefore, it is not possible to use two-terminal fault-location methods to locate the fault on the transmission line, unless by utilizing the model of the UPFC [6]. In this manner, the voltage and current of bus E are estimated by using the obtained data of bus B, that inserts inherent errors in the fault-location algorithm which are related to the UPFC model. In this paper, the presented method uses the known data to find the fault location and does not need to know the UPFC parameters, but uses the average power flow through the UPFC to determine the fault location. Thus, consider the average power of bus $B(P^B_{\rm Avg})$, which is shown in Fig. 1. It can be calculated by using the voltage and current vectors of bus $\mathbf{B}(\mathbf{v_B}, \mathbf{i_B})$ which are known. The average power of bus $E(P^E_{\rm Avg})$ can be obtained as follows:

$$P^E_{\rm Avg}(t) = P^B_{\rm Avg}(t) - \Delta p(t) \tag{1}$$

where

Δp absorbed or generated or lost average power by the UPFC.

Δp depends on three items:

1) resistive losses of series and shunt transformers and resistive losses of power-electronic switches of series and shunt converters of the UPFC;
2) absorbed or generated average power of the series and shunt transformers;
3) absorbed or generated or lost average power of the dc-link capacitor.

$\Delta p(t)$ depends on the UPFC operational characteristics and its controller system performance. Thus, $\Delta p(t)$ is related to the UPFC modeling but, it is negligible compared with $P^B_{\rm Avg}(t)$. By ignoring $\Delta p(t)$, $P^E_{\rm Avg}(t)$ is determined by means of $P^B_{\rm Avg}(t)$ and the fault-location method will be independent of the UPFC model. In Section III-C. it will be seen that ignoring $\Delta p(t)$ has no considerable effect on the results of the fault-location algorithm.

In this paper, the proposed algorithm uses the voltage and current of bus S and the average power of bus E to find the location of fault which is described in the following subsections. When the fault occurs on the right-hand side of the UPFC, the same procedure is performed.

At first, the basic principle of the proposed algorithm is described via the SE part of the transmission line for a symmetrical three-phase fault in the next subsection. Then, this algorithm is developed for the transmission line including the UPFC.

A. Symmetrical Three-Phase Fault

Fig. 2 shows the single-line diagram of the SE section of the transmission line. It is assumed that the sending end voltage and current vectors $(\mathbf{v_S}, \mathbf{i_S})$ and the average power of bus $\mathrm{E}(P^E_{\rm Avg})$ are known and available in the time domain; and the voltage and current vectors of bus $\mathrm{E}(\mathbf{v_E}, \mathbf{i_E})$ are unknown. For the kth mode ($k = 0$, 1 and 2), modal voltage and current components [10] at the left-hand side of the fault point $\left(v^{(k)}_{FS}, i^{(k)}_{FS}\right)$ can be written as a function of sending end modal components as follows [4]:

$$\begin{aligned} v^{(k)}_{\rm FS}(t) = \Bigg(& (Z'^{(k)}_{\rm Sc})^2[v^{(k)}_S(t+\tau^{(k)}) - Z'^{(k)}_{\rm Sc} i^{(k)}_S(t+\tau^{(k)})] \\ & + (Z''^{(k)}_{\rm Sc})^2[v^{(k)}_S(t-\tau^{(k)}) + Z''^{(k)}_{\rm Sc} i^{(k)}_S(t-\tau^{(k)})] \\ & - \frac{Z'^{(k)}_{\rm Sc} R^{(k)}_S}{4}.\left[\frac{\frac{R^{(k)}_S}{2}}{Z'^{(k)}_{\rm Sc}}.v^{(k)}_S(t) + 2Z''^{(k)}_{\rm Sc} i^{(k)}_S(t)\right]\Bigg) \Bigg/ 2(Z^{(k)}_c)^2 \end{aligned} \tag{2}$$

$$\begin{aligned} i^{(k)}_{\rm FS}(t) = \Bigg(& Z'^{(k)}_{\rm Sc}[v^{(k)}_S(t+\tau^{(k)}) - Z'^{(k)}_{\rm Sc} i^{(k)}_S(t+\tau^{(k)})] \\ & - Z^{(k)}_{\rm Sc}[v^{(k)}_S(t-\tau^{(k)}) + Z^{(k)}_{\rm Sc} i^{(k)}_S(t-\tau^{(k)})] \\ & - \frac{R^{(k)}_S}{4}.\left[2.v^{(k)}_S(t) - \frac{R^{(k)}_S}{2} i^{(k)}_S(t)\right]\Bigg) \Bigg/ 2(Z^{(k)}_c)^2 \end{aligned} \tag{3}$$

where

$\tau^{(k)}$ kth-mode elapsed time for the wave propagation from the sending end to the fault point;

$Z^{(k)}_c$ kth mode characteristic impedance;

$R^{(k)}_S$ kth mode line resistance from S to F.

$$Z'^{(k)}_{\rm Sc} = \frac{Z^{(k)}_c + R^{(k)}_S}{4}$$
$$Z''^{(k)}_{\rm Sc} = \frac{Z^{(k)}_c - R^{(k)}_S}{4}.$$

Because of line continuity and consequently voltage continuity along the line, the voltage vectors at the right- and left-hand side of the fault point are equal $(\mathrm{v_{FE}} = \mathrm{v_{FS}})$. So the following relation is expressed at the fault point using the Kirchhoff's current law for the kth mode:

$$i^{(k)}_{\rm FE}(t) = -i^{(k)}_{\rm FS}(t) - \frac{v^{(k)}_{\rm FS}(t)}{R_f} \tag{4}$$

where

R_f fault resistance;

$i_{\mathrm{FE}}^{(k)}(t)$ kth-mode current component at the right-hand side of the fault point.

The modal voltage and current components at the left-hand side of bus E $\left(v_E^{(k)}, i_E^{(k)}\right)$ can be written as a function of the modal voltage and current components at the right-hand side of the fault point by using the distributed parameters of the line model. Thus, the following equations can be obtained according to Fig. 2 [4]:

$$\begin{aligned} v_E^{(k)}(t) = \Bigg(& (Z_{\mathrm{Ec}}'^{(k)})^2 [v_{\mathrm{FE}}^{(k)}(t+\tau_{\mathrm{SE}}^{(k)}-\tau^{(k)}) \\ & - Z_{\mathrm{Ec}}'^{(k)} i_{\mathrm{FE}}^{(k)}(t+\tau_{\mathrm{SE}}^{(k)}-\tau^{(k)})] \\ & + (Z''^{(k)}_{\mathrm{Ec}})^2 [v_{\mathrm{FE}}^{(k)}(t-\tau_{SE}^{(k)}+\tau^{(k)}) + Z''^{(k)}_{\mathrm{Ec}} i_{\mathrm{FE}}^{(k)}(t-\tau_{SE}^{(k)}+\tau^{(k)})] \\ & - \frac{Z_{\mathrm{Ec}}'^{(k)} R_E'^{(k)}}{4} \cdot \left[\frac{\frac{R_E'^{(k)}}{2}}{Z_{\mathrm{Ec}}'^{(k)}} . v_{\mathrm{FE}}^{(k)}(t) + 2 Z''^{(k)}_{\mathrm{Ec}} i_{\mathrm{FE}}^{(k)}(t) \right] \Bigg) \Bigg/ 2(Z_c^{(k)})^2 \end{aligned} \tag{5}$$

$$\begin{aligned} i_E^{(k)}(t) = \Bigg(& Z_{\mathrm{Ec}}'^{(k)} [v_{\mathrm{FE}}^{(k)}(t+\tau_{\mathrm{SE}}^{(k)}-\tau^{(k)}) \\ & - Z_{\mathrm{Ec}}'^{(k)} i_{\mathrm{FE}}^{(k)}(t+\tau_{\mathrm{SE}}^{(k)}-\tau^{(k)})] \\ & - Z''^{(k)}_{\mathrm{Ec}} [v_{\mathrm{FE}}^{(k)}(t-\tau_{\mathrm{SE}}^{(k)}+\tau^{(k)}) + Z''^{(k)}_{\mathrm{Ec}} i_{\mathrm{FE}}^{(k)}(t-\tau_{\mathrm{SE}}^{(k)}+\tau^{(k)})] \\ & - \frac{R_E^{(k)}}{4} \cdot \left[2 v_{\mathrm{FE}}^{(k)}(t) - \frac{R_E^{(k)}}{2} i_{\mathrm{FE}}^{(k)}(t) \right] \Bigg) \Bigg/ 2(Z_c^{(k)})^2 \end{aligned} \tag{6}$$

where

$R_E^{(k)}$ kth-mode line resistance from bus E to F;

$\tau_{\mathrm{SE}}^{(k)}$ kth-mode elapsed time for the wave propagation from bus S to E.

$$Z_{\mathrm{Ec}}'^{(k)} = \frac{Z_c^{(k)} + R_E^{(k)}}{4}, \quad Z\mathrm{Ec}^{(k)} = \frac{Z_c^{(k)} - R_E^{(k)}}{4}.$$

By substituting (4) into (5) and (6), (7) and (8) are derived, respectively: See (7) and (8) at the bottom of the page.

By substituting (2) and (3) into (7) and (8), the kth-mode voltage and current components of bus E $\left(v_E^{(k)}, i_E^{(k)}\right)$ are obtained as a function of the kth-mode voltage and current components of the sending end $\left(v_S^{(k)}, i_S^{(k)}\right)$, the kth-mode elapsed time for the wave propagation from S to F $(\tau^{(k)})$ and the fault resistance (R_f)

$$v_E^{(k)}(t) = g_1\left(v_S^{(k)}, i_S^{(k)}, \tau^{(k)}, R_f, t\right) \tag{9}$$

$$i_E^{(k)}(t) = f_1\left(v_S^{(k)}, i_S^{(k)}, \tau^{(k)}, R_f, t\right). \tag{10}$$

$\tau^{(k)}$ is proportional to the fault distance from the sending end (x), thus

$$v_E^{(k)}(t) = g_1\left(v_S^{(k)}, i_S^{(k)}, x, R_f, t\right) \tag{11}$$

$$i_E^{(k)}(t) = f_1\left(v_S^{(k)}, i_S^{(k)}, x, R_f, t\right). \tag{12}$$

The average power of bus E over a period of time T is formulated as

$$P_{\mathrm{Avg}}^E(t) = \frac{1}{T} \int_{t-T}^{t} [\mathbf{v_E}(t_1)]' . \mathbf{i_E}(t_1) . dt_1 \tag{13}$$

$$\begin{aligned} v_E^{(k)}(t) = \Bigg(& (Z_{\mathrm{Ec}}'^{(k)})^2 \left[\left(1 + \frac{Z_{\mathrm{Ec}}'^{(k)}}{R_f} \right) . v_{\mathrm{FS}}^{(k)}(t+\tau_{\mathrm{SE}}^{(k)}-\tau^{(k)}) + Z_{\mathrm{Ec}}'^{(k)} i_{\mathrm{FS}}^{(k)}(t+\tau_{\mathrm{SE}}^{(k)}-\tau^{(k)}) \right] \\ & + (Z''^{(k)}_{\mathrm{Ec}})^2 \left[\left(1 - \frac{Z''^{(k)}_{\mathrm{Ec}}}{R_f} \right) . v_{\mathrm{FS}}^{(k)}(t-\tau_{\mathrm{SE}}^{(k)}+\tau^{(k)}) - Z''^{(k)}_{\mathrm{Ec}} i_{\mathrm{FS}}^{(k)}(t-\tau_{\mathrm{SE}}^{(k)}+\tau^{(k)}) \right] \\ & - \frac{Z_{\mathrm{Ec}}'^{(k)} R_E^{(k)}}{4} \cdot \left[\left(\frac{\frac{R_E^{(k)}}{2}}{Z_{\mathrm{Ec}}'^{(k)}} - \frac{2 Z_{\mathrm{Ec}}'^{(k)}}{R_f} \right) . v_{\mathrm{FS}}^{(k)}(t) - 2 Z''^{(k)}_{\mathrm{Ec}} i_{\mathrm{FS}}^{(k)}(t) \right] \Bigg) \Bigg/ 2(Z_c^{(k)})^2 \end{aligned} \tag{7}$$

$$\begin{aligned} i_E^{(k)}(t) = \Bigg(& Z_{\mathrm{Ec}}'^{(k)} \left[\left(1 + \frac{Z_{\mathrm{Ec}}'^{(k)}}{R_f} \right) . v_{\mathrm{FS}}^{(k)}(t+\tau_{\mathrm{SE}}^{(k)}-\tau^{(k)}) + Z_{\mathrm{Ec}}'^{(k)} i_{\mathrm{FS}}^{(k)}(t+\tau_{\mathrm{SE}}^{(k)}-\tau^{(k)}) \right] \\ & - Z''^{(k)}_{\mathrm{Ec}} \left[\left(1 - \frac{Z''^{(k)}_{\mathrm{Ec}}}{R_f} \right) . v_{\mathrm{FS}}^{(k)}(t-\tau_{\mathrm{SE}}^{(k)}+\tau^{(k)}) - Z''^{(k)}_{\mathrm{Ec}} i_{\mathrm{FS}}^{(k)}(t-\tau_{\mathrm{SE}}^{(k)}+\tau^{(k)}) \right] \\ & - \frac{R_E^{(k)}}{4} \cdot \left[\left(2 + \frac{R_E^{(k)}}{2.R_f} \right) . v_{\mathrm{FS}}^{(k)}(t) + \frac{R_E^{(k)}}{2} i_{\mathrm{FS}}^{(k)}(t) \right] \Bigg) \Bigg/ 2(Z_c^{(k)})^2 . \end{aligned} \tag{8}$$

where

$\mathbf{v_E}(t)$, $\mathbf{i}_{\mathrm{E}}(t)$ third-order column vectors representing actual phase voltages and currents of bus E.

By applying the Karrenbauer transformation [10] to (11) and (12), the modal voltages and currents are transformed to the phase voltage and current vectors. Then, by substituting the obtained results into (13), along with rearranging it, the following nonlinear equation is derived:

$$(-P^{E}_{\mathrm{Avg}}(t) + h_1(\mathbf{v_S}, \mathbf{i_S}, x, t)) * R_f^2 + h_2(\mathbf{v_S}, \mathbf{i_S}, x, t) * R_f + h_3(\mathbf{v_S}, \mathbf{i_S}, x, t) = 0 \quad (14)$$

where h_1, h_2, and h_3 are functions of the time, the sending end voltage, and current vectors and the fault distance from bus $S(x)$. Equation (14) has two unknown variables (i.e., x and R_f). By solving (14), the fault location and the fault resistance are calculated. It should be noted that the nonlinear (14) is a quadratic equation with respect to R_f.

Hitherto, an important part of the proposed method is described via the SE section of the line assuming that the sending end voltage and current vectors and the average power of bus E are known and available. This part of the method is subsequently used to develop the fault-location algorithm for transmission lines including the UPFC.

B. Transmission Lines Including UPFC

Since the location of fault with respect to the UPFC location is unknown prior to estimation of the fault location, three steps are considered to describe the method. In the first and second steps, it is assumed that the fault is located on the left- and right-hand side of the UPFC, respectively. Two quadratic equations with respect to the first two steps are obtained, which are finally used to derive an optimization problem in the third step. The correct location of fault is achieved by solving the obtained optimization problem. These steps are illustrated as follows.

Step 1) In this step, it is assumed that a three-phase fault occurs on the left-hand side of the UPFC (as shown in Fig. 1). Thus, the described procedure in Section II-A can be utilized. The BR section of the line is sound. So the voltage and current vectors at the right-hand side of the UPFC $(\mathbf{v_B}, \mathbf{i_B})$ can be obtained by using the receiving end voltage and current vectors $(\mathbf{v_R}, \mathbf{i_R})$

$$\mathbf{v_B}(t) = g_2(\mathbf{v_R}, \mathbf{i_R}, t) \quad (15)$$

$$\mathbf{i_B}(t) = f_2(\mathbf{v_R}, \mathbf{i_R}, t). \quad (16)$$

Based on (1) and ignoring $\Delta p(t)$, the average power of bus $E(P^{E}_{\mathrm{Avg}}(t))$ is equal to which is defined as follows:

$$P^{B}_{\mathrm{Avg}}(t) = \frac{1}{T}\int_{t-T}^{t} [\mathbf{v_B}(t_1)]'.\mathbf{i_B}(t_1).dt_1. \quad (17)$$

By substituting (15) and (16) into (17), and then by substituting the result into (14), the following quadratic equation with respect to R_f is obtained:

$$\begin{cases} H_1(\mathbf{v_S}, \mathbf{i_S}, \mathbf{v_R}, \mathbf{i_R}, x, R_f, t) = A_1 * R_f^2 + B_1 * R_f + C_1 = 0 \\ 0 < x < x_{SE} \end{cases} \quad (18)$$

where

x_{SE} distance of bus E from the sending end.

$$A_1 = h_1 - \frac{1}{T}\int_{t-T}^{t} [g_2]'.f_2.dt_1$$
$$B_1 = h_2$$
$$C_1 = h_3.$$

Equation (18) is derived assuming that the fault occurs on the first part of the line (SE section). So it is valid for $0 < x < x_{\mathrm{SE}}$..

Step 2) In this step, it is assumed that the fault is located on the right-hand side of the UPFC and the SE section of the line is sound. The voltage and current vectors at the left-hand side of the UPFC $(\mathbf{v_E}, \mathbf{i_E})$ can be obtained by using the sending end voltage and current vectors $(\mathbf{v_S}, \mathbf{i_S})$. So the following equations can be expressed like (15) and (16):

$$\mathbf{v_E}(t) = g_3(\mathbf{v_S}, \mathbf{i_S}, t) \quad (19)$$

$$\mathbf{i_E}(t) = f_3(\mathbf{v_S}, \mathbf{i_S}, t). \quad (20)$$

By ignoring Δp in (1), the average power of bus B $(P^{B}_{\mathrm{Avg}}(t))$ is equal to $P^{E}_{\mathrm{Avg}}(t)$. Considering the BR part of the line, the average power of bus B $(P^{B}_{\mathrm{Avg}}(t))$ is known and the voltage and current vectors of bus R are available. Therefore, the described procedure in Section II-A can be employed again. Thus, by using (19) and (20), the following equation is derived similar to (18):

$$\begin{cases} H_2(\mathbf{v_S}, \mathbf{i_S}, \mathbf{v_R}, \mathbf{i_R}, x, R_f, t) = A_2 * R_f^2 + B_2 * R_f + C_2 = 0 \\ x_{\mathrm{SE}} < x < x_{SR} \end{cases} \quad (21)$$

where

x_{SR} distance of bus R from S, A_2, B_2 and C_2 can be derived similar to A_1, B_1, and C_1, respectively.

Equation (21) is obtained for the fault on the BR section of the line so $x_{\mathrm{SE}} < x < x_{\mathrm{SR}}$.

Equations (18) and (21) are utilized to derive the optimization problem in the next step.

Step 3) double-criterion function (22) is defined based on (18) and (21), which are obtained in the first and second steps

$$H = \begin{cases} H_1(\mathbf{v_S}, \mathbf{i_S}, \mathbf{v_R}, \mathbf{i_R}, x, R_f, t) & 0 < x < x_{\rm SE} \\ H_2(\mathbf{v_S}, \mathbf{i_S}, \mathbf{v_R}, \mathbf{i_R}, x, R_f, t) & x_{\rm SE} < x < x_{\rm SR} \end{cases}. \tag{22}$$

Function (22) is valid for all points of the line from the beginning to the end, except for the UPFC location. But just at the true fault point and for the true fault resistance, function (22) is equal to zero during the fault occurrence

$$\begin{cases} H(\mathbf{v_S}, \mathbf{i_S}, \mathbf{v_R}, \mathbf{i_R}, x, R_f, t) = 0 \\ 0 < x < x_{\rm SR}, \\ \quad x \neq x_{\rm SE} \end{cases} \tag{23}$$

In (23), only two unknown variables exist: the fault distance from the sending end (x) and the fault resistance (R_f). To find the location and resistance of the fault, at first (23) is discretized

$$\begin{cases} H(\mathbf{v_S}, \mathbf{i_S}, \mathbf{v_R}, \mathbf{i_R}, x, R_f, n) = 0 \\ 0 < x < x_{SR}, \\ \quad x \neq x_{SE} \end{cases} \tag{24}$$

where

$n.\Delta t = t$;

Δt sampling step;

n arbitrary integer.

The samples in the fault interval data window should satisfy this equation. Thus, the fault-location problem is converted to an optimization one and the following optimization problem is expressed based on discretized (24):

$$\begin{cases} \mathrm{MinJ(x, R_f)} = \underset{\mathrm{x,R_f}}{\mathrm{Min}} \sum_{\mathrm{n}} \mathrm{H}(\mathbf{v_S}, \mathbf{i_S}, \mathbf{v_R}, \mathbf{i_R}, \mathrm{x, R_f, n}) \\ \text{Subject to:} \begin{cases} 0 \leq R_f \\ 0 < x < x_{\rm SR} \\ \quad x \neq x_{SE}. \end{cases} \end{cases} \tag{25}$$

Since the fault resistance is a positive number, the constraint $R_f \leq 0$ is added to the optimization problem. Solving optimization problem (25)[11], it offers the solution (x_F, R_F), where x_F is the obtained location of fault and R_F is the obtained fault resistance. Therefore, the location of fault and the correct side of it are determined simultaneously.

Since search point x is limited to the line length, this optimization problem can be solved using the enumeration method [11]. Thus, the objective function values are calculated for all x values along the line by a step of Δx. Then, the minimum of the objective function values is chosen to solve the problem and find the fault location. Thus, set $x_1 = \Delta x$, now (18) has one unknown quantity (i.e., R_f). Using the least square estimation method, the fault resistance $R_{\rm f1}$ is achieved from (18) for x_1, and the objective function value $J(x_1, R_{\rm f1})$ is calculated by using (25). Then, x is increased to $x_2 = 2\Delta x$ by the step of Δx and (18) is solved again using the least square estimation method, and the objective function value $J(x_2, R_{\rm f2})$ is calculated by using (25) for x_2. This procedure is continued until $x = x_{\rm SE}$ and the objective function values are calculated for all x values within the span of $0 < x < x_{\rm SE}$. The same procedure is performed for the second part of the line $(x_{\rm SE} < x < x_{\rm SR})$, but the difference is that (21) is utilized instead of (18). Hitherto, the objective function values are calculated for all x values within the span of $0 < x < x_{\rm SR}$. Now the optimization problem is solved by choosing the minimum of these values. It is worth noting that after obtaining the minimum of the objective function values and determining the location of the fault, the fault side is also identified and employing a selector is not required.

As seen from (25), only the sending and receiving end recorded data are needed to solve the optimization problem and they do not depend on the UPFC model. So the method does not need any information about the UPFC, operation of its control system, and controller parameters. In addition, this algorithm does not need to propose a selector to select the fault section with respect to the UPFC location. These are the salient advantages of the proposed algorithm.

The derivation procedure outlined previously for the symmetrical three-phase fault is applicable to every fault type but the difference exists in (4). For any fault type, at the fault point, by using Kirchhoff's current law; a set of equations is obtained like (4), and it should be employed instead of (4). Thus, the solutions for the other fault types can be similarly derived.

III. Testing and Evaluating

A. Studied System

A 300-km, 500-kV transmission line including a UPFC (shown in Fig. 1) was simulated in MATLAB/Simulink to evaluate the accuracy of the proposed algorithm. The parameters of the simulated system are presented in the Appendix. For the simulation study, the UPFC consists of two 200-MVA, three-level, 48-pulse voltage-source inverters which are connected through two 5000-μF capacitors as the dc link. The shunt inverter is connected to the transmission line through four 125/15-kV zigzag transformers and regulates the voltage at its point of connection to $V_{\rm ref}$, during steady-state operating conditions by controlling the absorbed or generated reactive power to the system, while also allowing active power transfer to the series converter through the dc link. Another inverter is connected to the transmission line through four 12.5/12.5-kV Zigzag transformers to regulate the active and reactive power flow through the transmission line.

B. Control System of the UPFC

Two parts are considered to model the control system of the UPFC for simulation in MATLAB/Simulink: the STATCOM control part and SSSC control part. The three-phase voltages at the STATCOM connecting point are sent to the phase-locked loop (PLL) to calculate the reference angle which is synchronized to the phase A voltage.

In the STATCOM control part, the three-phase shunt currents are decomposed into their real component $I_{\rm d}$ and reactive component $I_{\rm q}$ via the abc–dqo transformation using the

PLL angle as reference. The magnitude of the positive-sequence part of the connecting point voltage is compared with the reference voltage $V_{\rm ref}$, and the error is passed through a proportional-integral (PI) controller to produce the reference reactive current $I_{\rm qref}$. This current reference is compared with the reactive part of the shunt current to produce the error which will be passed through another PI controller to obtain the relative phase angle of the inverter voltage with respect to the phase A voltage. The phase angle, along with the PLL signal, is fed to the STATCOM firing pulse generator to generate the desired pulse for the voltage-source inverter.

For the SSSC, the series-injected voltage is determined by a closed-loop control system to ensure that the desired active and reactive powers flowing in the transmission line are maintained. The three-phase voltages and currents of bus B are decomposed into their direct and quadrature components via the abc–dqo transformation using the PLL angle as reference. The direct and quadrature components of the voltage of bus B, together with the desired $P_{\rm ref}$ and $Q_{\rm ref}$, are used to compute the desired real and reactive components of the line current $(I_{\rm prefL}, I_{\rm qrefL})$. These current references are compared with the active and reactive components of the line current to produce the errors which will be passed through two PI controllers to obtain the direct and quadrature components of the series converter voltage ($V_{\rm d}$ and $V_{\rm q}$), respectively. The magnitude and phase angle of the series converter voltage can be obtained by a rectangular to polar transformation of $V_{\rm d}$ and $V_{\rm q}$ components. The phase angle and dead angle (calculated using the relationship between the inverter voltage and the dc-link voltage), along with the PLL signal, are fed to the SSSC firing pulse generator to generate the desired pulse for the SSSC voltage-source inverter.

C. Simulation Results

To evaluate the accuracy of the proposed method, the error of the fault location is expressed in terms of the percentage of the total line length as follows:

$$\%\text{Error} = \frac{\text{Calculated distance} - \text{Actual distance}}{\text{Line length}} * 100. \quad (26)$$

As an example, a three-phase fault occurs at the distance of 200 km from the sending end. Its resistance is assumed to be 10 Ω, while the UPFC is installed at 150 km from the sending end and $P_{\rm ref} = 800$ MW and $Q_{\rm ref} = -100$ MVAr. The result of running the algorithm [by solving the obtained optimization problem (25)] is

$$(x_F, R_F) = (199.856\ \text{km},\ 9.759\ \Omega).$$

So the fault-location error is -0.0479%.

The accuracy of the algorithm is also evaluated under different operating conditions of the UPFC and various fault conditions, such as different fault locations (30, 80, 130, 180, 220, 280 km from the sending end), fault types (a-g, abc-g, ab-g, and ab fault), fault inception angles (0, 45, and 90°) and fault resistances (1, 10, and 30 Ω). The obtained results are shown in Tables I–VI.

Table I shows the fault-location results when the desired active power of the UPFC $(P_{\rm ref})$ is adjusted to 550 MW and the desired reactive power $(Q_{\rm ref})$ to -150 MVAr, and the voltage of the UPFC bus become 1.0095 p.u. before fault inception. The fault inception angle (IncAn) is assumed to be 90°. As an example, regarding this table, when the fault occurs at 280 km from the sending end, the fault location error is 0.0601%.

TABLE I
RESULTS OF COMPUTING THE FAULT LOCATION FOR DIFFERENT FAULT CONDITIONS

Fault type	Actual location of fault (km)	R_f=1Ω	R_f=10Ω	R_f=30Ω
		Fault Location Error (%)		
Single-phase to ground	30	0.2996	0.2996	0.2996
	80	0.2517	0.2517	0.2517
	130	0.2038	0.2038	0.2038
	180	-0.7674	-0.7674	-0.7674
	220	-0.2517	-0.2517	-1.175
	280	0.0601	0.0601	-0.8632
Three-phase to ground	30	0.2996	0.2996	0.2996
	80	0.2517	0.2517	0.2517
	130	0.2038	0.2038	0.2038
	180	0.1559	0.1559	0.1559
	220	-0.2517	-0.2517	-0.2517
	280	0.0601	0.0601	0.0601
Double-phase to ground	30	0.2996	0.2996	1.2229
	80	0.2517	0.2517	1.175
	130	0.2038	0.2038	1.1271
	180	0.1559	0.1559	-0.767
	220	-0.2517	-0.2517	-0.2517
	280	0.0601	0.0601	0.9833
Double-phase	30	0.2996	0.2996	-0.6236
	80	0.2517	0.2517	0.2517
	130	0.2038	0.2038	0.2038
	180	0.1559	0.1559	0.1559
	220	-0.2517	-0.2517	-0.2517
	280	0.0601	0.0601	0.0601

IncAn=90°, $P_{\rm ref}$=550MW, $Q_{\rm ref}$=-150MVAr

TABLE II
DETERMINING THE LOCATION OF THE FAULT FOR DIFFERENT FAULT INCEPTION ANGLES

Fault type	Actual location of fault (km)	IncAn=0°	IncAn=45°	IncAn=90°
		Fault Location Error (%)		
Single-phase to ground	30	0.2996	0.2996	0.2996
	80	-0.6715	0.2517	-0.6715
	130	-0.719	0.2038	0.2038
	180	0.1559	-0.7674	0.1559
	220	0.6715	-0.2517	-0.2517
	280	0.0601	0.0601	0.0601
Three-phase to ground	30	0.2996	0.2996	0.2996
	80	0.2517	0.2517	0.2517
	130	0.2038	0.2038	0.2038
	180	0.1559	0.1559	0.1559
	220	-0.2517	-0.2517	-0.2517
	280	0.0601	0.0601	0.0601
Double-phase to ground	30	0.2996	0.2996	0.2996
	80	0.2517	0.2517	1.175
	130	0.2038	0.2038	0.2038
	180	-0.767	0.1559	-0.7674
	220	-0.2517	-0.2517	-0.2517
	280	0.0601	-0.8632	-0.8632
Double-phase	30	0.2996	0.2996	0.2996
	80	0.2517	0.2517	0.2517
	130	0.2038	0.2038	0.2038
	180	0.1559	0.1559	0.1559
	220	-0.2517	-0.2517	-0.2517
	280	-0.8632	0.0601	0.0601

$P_{\rm ref}$=650MW, $Q_{\rm ref}$=100MVAr, R_f=10Ω

TABLE III
ERRORS OF FAULT-LOCATION COMPUTATION FOR DIFFERENT FAULT CONDITIONS

Fault type	Actual location of fault (km)	R_f=1Ω	R_f=10Ω	R_f=30Ω
		Fault location error (%)		
Single-phase to ground	30	0.2996	0.2996	1.2229
	80	0.2517	0.2517	0.2517
	130	0.2038	0.2038	-0.7194
	180	0.1559	-0.7674	-0.7674
	220	-0.2517	0.6715	-1.175
	280	0.0601	0.0601	0.9833
Three-phase to ground	30	0.2996	0.2996	0.2996
	80	0.2517	0.2517	0.2517
	130	0.2038	0.2038	0.2038
	180	0.1559	0.1559	0.1559
	220	-0.2517	-0.2517	-0.2517
	280	0.0601	0.0601	0.0601
Double-phase to ground	30	0.2996	0.2996	0.2996
	80	0.2517	0.2517	0.2517
	130	0.2038	0.2038	0.2038
	180	-0.767	0.1559	0.1559
	220	-0.2517	-0.2517	-0.2517
	280	0.0601	0.0601	0.0601
Double-phase	30	0.2996	0.2996	0.2996
	80	0.2517	0.2517	0.2517
	130	0.2038	0.2038	0.2038
	180	0.1559	0.1559	0.1559
	220	-0.2517	-0.2517	-0.2517
	280	0.0601	0.0601	0.0601

IncAn=45°, P_{ref}=750MW, Q_{ref}=-50MVAr

However, the absolute error of the fault location increases to 1.2229% when the double-phase-to-ground fault occurs at 30 km from bus S with $R_f = 30\ \Omega$.

Table II provides the errors of the fault-location computation for different fault conditions while the reference active power of the UPFC (P_{ref}) is changed to 650 MW and the reference reactive power (Q_{ref}) to 100 MVAr, and the prefault voltage of the UPFC bus is 0.9914 p.u. In this case, the fault inception angles (IncAn) are considered to be 0, 45, and 90°, and the fault resistance is 10 Ω. As shown in Table II, the absolute error of the fault location varies between 0.0601% and 1.175%. The maximum absolute error is obtained for the double-phase-to-ground fault at 80 km from the sending end, while $\text{IncAn} = 90°$.

The reference active power of the UPFC is changed to 750 MW and the reference reactive power to −50 MVAr; thus, the prefault voltage of the UPFC bus alters to 1.0027 p.u. The fault inception angle is chosen to be 45° and the fault-location determination errors in percentage are depicted in Table III for various fault conditions. The presented results in this table show that the maximum absolute error is 1.2229% for the single-phase-to-ground fault at 30 km from the sending end, when $R_f = 30\ \Omega$.

Table IV depicts the fault-location results for different references of the active and reactive power flow of the UPFC for two locations of the fault (100 km and 230 km from the sending end). The single-phase-to-ground fault is considered, and its resistance is chosen as 1 and 30 Ω. The fault inception angle is assumed to be 90° in these cases. In Table IV, the minimum absolute error is 0.048%. It can also be seen that the maximum absolute error is 0.815% while $P_{\text{ref}} = 700$ MW and $Q_{\text{ref}} = 100$ MVAr, and the fault resistance is 30 Ω when the fault occurs at 230 km from the sending end.

TABLE IV
ERRORS OF FAULT-LOCATION COMPUTATION FOR DIFFERENT SETTINGS OF THE UPFC

Active and reactive power references (MW, MVAr)	Actual location of fault (km)	R_f=1Ω		R_f=30Ω	
		Calculated location of fault (km)	Error (%)	Calculated location of fault (km)	Error (%)
P_{ref}=600, Q_{ref}=-200	100	100.1437	0.048	100.1437	0.048
	230	230.324	0.108	230.324	0.108
P_{ref}=600, Q_{ref}=-150	100	100.1437	0.048	100.1437	0.048
	230	230.324	0.108	230.324	0.108
P_{ref}=600, Q_{ref}=-100	100	100.1437	0.048	100.1437	0.048
	230	230.324	0.108	230.324	0.108
P_{ref}=600, Q_{ref}=0	100	100.1437	0.048	100.1437	0.048
	230	230.324	0.108	230.324	0.108
P_{ref}=700, Q_{ref}=-200	100	100.1437	0.048	100.1437	0.048
	230	230.324	0.108	230.324	0.108
P_{ref}=700, Q_{ref}=-150	100	100.1437	0.048	100.1437	0.048
	230	230.324	0.108	230.324	0.108
P_{ref}=700, Q_{ref}=-100	100	100.1437	0.048	100.1437	0.048
	230	230.324	0.108	230.324	0.108
P_{ref}=700, Q_{ref}=0	100	100.1437	0.048	100.1437	0.048
	230	230.324	0.108	230.324	0.108
P_{ref}=700, Q_{ref}=100	100	100.1437	0.048	100.1437	0.048
	230	230.324	0.108	227.554	-0.815
P_{ref}=800, Q_{ref}=-150	100	100.1437	0.048	100.1437	0.048
	230	230.324	0.108	230.324	0.108
P_{ref}=800, Q_{ref}=-100	100	100.1437	0.048	100.1437	0.048
	230	230.324	0.108	230.324	0.108
P_{ref}=800, Q_{ref}=0	100	100.1437	0.048	100.1437	0.048
	230	230.324	0.108	230.324	0.108
P_{ref}=800, Q_{ref}=100	100	100.1437	0.048	100.1437	0.048
	230	230.324	0.108	230.324	0.108

IncAn=90°

TABLE V
ERRORS OF FAULT-LOCATION COMPUTATION FOR DIFFERENT SERIES-INJECTED VOLTAGE MAGNITUDE OF THE UPFC

Series injected voltage magnitude (%)	Actual location of fault (km)	R_f=1Ω		R_f=30Ω	
		Calculated location of fault (km)	Error (%)	Calculated location of fault (km)	Error (%)
0	70	69.676	-0.108	72.445	0.815
	200	199.856	-0.048	199.856	-0.048
2	70	69.676	-0.108	72.445	0.815
	200	199.856	-0.048	199.856	-0.048
5	70	69.676	-0.108	72.445	0.815
	200	199.856	-0.048	199.856	-0.048
7	70	69.676	-0.108	72.445	0.815
	200	199.856	-0.048	199.856	-0.048
10	70	69.676	-0.108	72.445	0.815
	200	199.856	-0.048	199.856	-0.048
12	70	69.676	-0.108	72.445	0.815
	200	199.856	-0.048	199.856	-0.048
15	70	69.676	-0.108	72.445	0.815
	200	199.856	-0.048	199.856	-0.048

IncAn=90°

The effect of variation of the series-injected voltage magnitude of the UPFC is studied on the fault-location accuracy and some of the results are shown in Table V. In this table, the

TABLE VI
ERRORS OF FAULT-LOCATION COMPUTATION FOR DIFFERENT SERIES-INJECTED VOLTAGE PHASE ANGLES OF THE UPFC

Series injected voltage phase angle (degree)	Actual location of fault (km)	R_f=1Ω		R_f=30Ω	
		Calculated location of fault (km)	Error (%)	Calculated location of fault (km)	Error (%)
0	70	69.676	-0.108	69.676	-0.108
	200	199.856	-0.048	199.856	-0.048
35	70	69.676	-0.108	72.445	0.815
	200	199.856	-0.048	199.856	-0.048
90	70	69.676	-0.108	72.445	0.815
	200	199.856	-0.048	199.856	-0.048
135	70	69.676	-0.108	72.445	0.815
	200	199.856	-0.048	199.856	-0.048
180	70	69.676	-0.108	72.445	0.815
	200	199.856	-0.048	199.856	-0.048
270	70	69.676	-0.108	69.676	-0.108
	200	199.856	-0.048	199.856	-0.048
350	70	69.676	-0.108	69.676	-0.108
	200	199.856	-0.048	199.856	-0.048

IncAn=90°

single-phase-to-ground fault is considered at 70 km and 200 km from the sending end, and the fault resistances are assumed to be 1 Ω and 30 Ω while the fault inception angle is 90°. The fault-location error varies from −0.048% to 0.815% for different series-injected voltage magnitudes with variation from 0 to 15% with a phase angle of 57.3° (1 radian).

The accuracy of the algorithm is also evaluated by varying the series-injected voltage phase angle of the UPFC. Table VI depicts the fault-location errors when the series-injected voltage phase angle varies from 0 to 350° with a series voltage magnitude of 10%. In this table, the fault conditions are as in the previous case. The maximum absolute error is 0.815% where the fault occurs at 70 km from the sending end, and its resistance is assumed to be 30 Ω.

The fault-location errors presented in this paper have been compared with the existing study in [6]. The fault-location errors reported in [6] are within 3–4% for average operating conditions, whereas in the presented study, as concluded from Tables I–IV, the absolute of the fault-location error varies from 0.0479% to the maximum of 1.2229%.

In practice, the conventional instrument transformers may insert errors to measurements. For comprehensive evaluation, sensitivity analysis of the proposed algorithm to the measurement errors is carried out. Thus the voltage and current samples gathered from MATLAB/Simulink are subjected to perturbations, and then are fed into the proposed fault-location algorithm. This study is performed for various fault locations and types, and the fault resistance is assumed to be 10 Ω. During the first time, the voltage samples of buses S and R are perturbed by the error of +5%, and the current samples by −5%. Another time, these voltage and current samples are perturbed conversely (i.e., the errors of −5% and +5% are added to the voltage and current samples, respectively, and the results of running the proposed method in these cases are shown in Table VII). From this table, it can be seen that the maximum absolute error is 5.743% when the single-phase-to-ground fault occurs at 130 km from the sending end. It is worth noting that the perturbation errors have low influences in most cases.

TABLE VII
EFFECT OF MEASUREMENT ERRORS ON THE ACCURACY OF THE PROPOSED METHOD

Fault type	Actual location of fault (km)	+5% error in v_S and v_R, -5% error in i_S and i_R		-5% error in v_S and v_R, +5% error in i_S and i_R	
		Calculated location of fault (km)	Error (%)	Calculated location of fault (km)	Error (%)
Single-phase to ground	30	30.898	0.2996	28.129	-0.623
	80	80.755	0.2517	72.445	-2.518
	130	147.23	5.743	122.302	-2.566
	180	174.928	-1.690	186.007	2.00
	220	216.475	-1.175	224.784	1.594
	280	277.410	-0.8632	280.180	0.0601
Three-phase to ground	30	28.129	-0.6236	30.898	0.2996
	80	80.755	0.2517	75.215	-1.594
	130	130.611	0.2038	127.841	-0.7194
	180	180.467	0.1559	180.467	0.1559
	220	219.244	-0.2517	222.014	0.6715
	280	280.180	0.0601	280.180	0.0601
Double-phase to ground	30	33.668	1.2229	30.898	0.2996
	80	83.525	1.175	80.755	0.2517
	130	130.611	0.2038	130.611	0.2038
	180	180.467	0.1559	180.467	0.1559
	220	219.244	-0.2517	219.244	-0.2517
	280	277.410	-0.8632	280.180	0.0601
Double-phase	30	30.898	0.2996	30.898	0.2996
	80	80.755	0.2517	80.755	0.2517
	130	130.611	0.2038	130.611	0.2038
	180	180.467	0.1559	180.467	0.1559
	220	219.244	-0.2517	219.244	-0.2517
	280	280.180	0.0601	280.180	0.0601

IncAn=45°, P_{ref}=750MW, Q_{ref}=-50MVAr, R_f=10Ω

IV. CONCLUSION

In this paper, a novel fault-location algorithm for transmission lines, including UPFC, is proposed. In the presented method, synchronized data of two ends of transmission line are used, and the distributed parameter line model in the time domain is taken into account. The proposed method is composed of three steps. In the first two steps, assuming that the fault is located on the left- and right-hand side of the UPFC, two quadratic equations are obtained which are used to derive the optimization problem in the third step. The side and location of the fault and its resistance are determined simultaneously by solving this optimization problem; thus, the algorithm does not need to propose a selector. Also, the proposed method does not use the model of the UPFC for the fault location. So the accuracy of the proposed fault-location algorithm is not under influence of the UPFC modeling. A three-level, 48-pulse UPFC is considered for simulation in MATLAB/Simulink to evaluate the performance of the presented method. The simulation results show that the maximum absolute fault-location error does not exceed 1.2229% in the simulated cases without considering error in measurements. The sensitivity analysis of the proposed algorithm to the measurement errors is also performed. The results show that the perturbation errors have low effects in most cases.

APPENDIX

Power System: System nominal voltage: 500 (kV);
System nominal frequency: 60 (Hz);
Phase angle between voltage sources: 20°.

Transmission Line: Zero sequence: $R_0 = 0.275$ (Ω/km), $L_0 = 3.4505998$ (mH/km), $C_0 = 8.5$ (nF/km)
Positive sequence: $R_1 = 0.0275$ (Ω/km), $L_1 = 1.002768$ (mH/km), $C_1 = 13$ (nF/km)

REFERENCES

[1] Y. H. Song and A. T. Johns, *Flexible AC Transmission Systems (FACTS)*. London, U.K.: Inst. Elect. Eng., 1999.

[2] E. Acha, C. R. Fuerte-Esquivel, H. Ambriz-Perez, and C. Angeles-Camacho, *FACTS, Modelling and Simulation in Power Network*. Hoboken, NJ: Wiley, 2004.

[3] M. M. Saha, I. Izykowski, E. Rosolowski, and B. Kasztenny, "A new accurate fault locating algorithm for series compensated lines," *IEEE Trans. Power Del.*, vol. 14, no. 3, pp. 789–797, Jul. 1999.

[4] J. Sadeh, N. Hadjsaid, A. M. Ranjbar, and R. Feuillet, "Accurate fault location algorithm for series compensated transmission lines," *IEEE Trans. Power Del.*, vol. 15, no. 3, pp. 1027–1033, Jul. 2000.

[5] M. Al-Dabbagh and S. K. Kapuduwage, "Using instantaneous values for estimating fault locations on series compensated transmission lines," *Elect. Power Syst. Res.*, vol. 76, pp. 25–32, 2005.

[6] S. R. Samantaray, L. N. Tripathy, and P. K. Dash, "Differential equation-based fault locator for unified power flow controller-based transmission line using synchronised phasor measurements," *IET Gen., Transm. Distrib.*, vol. 3, no. 1, pp. 86–98, 2009.

[7] C.-S. Yu, C.-W. Liu, S.-L. Yu, and J.-A. Jiang, "A new PMU based fault location algorithm for series compensated lines," *IEEE Trans. Power Del.*, vol. 17, no. 1, pp. 33–46, Jan. 2002.

[8] J. Sadeh and A. Adinehzadeh, "Accurate fault location algorithm for transmission line in the presence of series connected FACTS devices," *Int. J. Elect. Power Energy Syst.*, vol. 32, no. 4, pp. 323–328, May 2010.

[9] M. Naghdi, J. Sadeh, and R. Ghazi, "Fault location in transmission lines compensated with shunt FACTS devices," presented at the 16th Iranian Conf. Elect. Eng., Tehran, Iran, 2008.

[10] A. T. Johns and S. K. Salman, *Digital Protection for Power Systems*. London, U.K.: Peregrinus Ltd., 1995.

[11] J. S. Arora, *Introduction to Optimum Design*. Boston, MA: Elsevier, 2004.

Mahdi Ghazizadeh Ahsaee received the B.Sc. degree in electronic engineering from Bahonar University of Kerman, Kerman, Iran, in 2000, the M.Sc. degree in electrical engineering from Mazandaran University, Babol, in 2003, and is currently pursuing the Ph.D. degree at Ferdowsi University of Mashhad, Mashhad.

Then, he served as a Scientific Member at the University of Zabol, Zabol, Iran. His current research interests are power system protection and the application of flexible ac transmission systems devices.

Javad Sadeh (M'08) received the B.Sc. and M.Sc. degrees (Hons.) in electrical engineering from Ferdowsi University of Mashhad, Mashhad, Iran, in 1990 and 1994, respectively and the Ph.D. degree in electrical engineering from Sharif University of Technology, Tehran, with the collaboration of the electrical engineering laboratory of the Institut National Polytechnique de Grenoble (INPG), Grenoble, France, in 2001.

Currently, he is an Associate Professor in the Department of Electrical Engineering, Ferdowsi University of Mashhad. His research interests are power system protection, dynamics, and operation.